Report
UCRL-ID-153650

Review of Rock Joint Models

J. P. Morris

June 17, 2003

Abstract

This report discusses several constitutive models for joint behavior with emphasis upon the experimental data which motivates them. Particular emphasis is placed upon data available for granite. The LDEC joint model is presented in detail and LDEC simulations using this model are compared against data from constant normal stiffness and constant normal load tests.

1 Review of Experimental Results for Shearing of Single Joints

1.1 Typical Shear Test Configurations

In order to discuss the models and experimental results we first need to establish in cartoon form what tests are typically performed on joints. Fig. 1 shows schematically two general types of shear test:

- Constant Normal Load (CNL): The joint is confined by a constant stress normal (σ_n) to the joint and measurements are conducted under increasing shear stress. Even if the joint dilates, the apparatus serves to maintain a constant normal load on the joint.

- Constant Normal Stiffness (CNS): The joint is confined by apparatus with prescribed stiffness (k_{rm}). If the joint has a tendency to dilate the normal stress (σ_n) will increase as the surrounding apparatus responds. Typically the joint is subjected to an initial normal stress (σ_{n0}).

1.2 Experimental Results for Granite

In this section we review *some* shear test data obtained on granite specimens.

Olsson and Barton [2001] obtained cores of granite drilled parallel to a joint plane in a naturally occurring joint rock mass. They performed shear tests under both constant normal load (CNL) and constant normal stiffness (CNS). They provide shear stress versus shear displacement and normal displacement versus shear displacement data.

Obert et al. [1976] considered intact, induced-fractured and sawed samples of granite and sandstone. We will only consider their results for fractured granite.

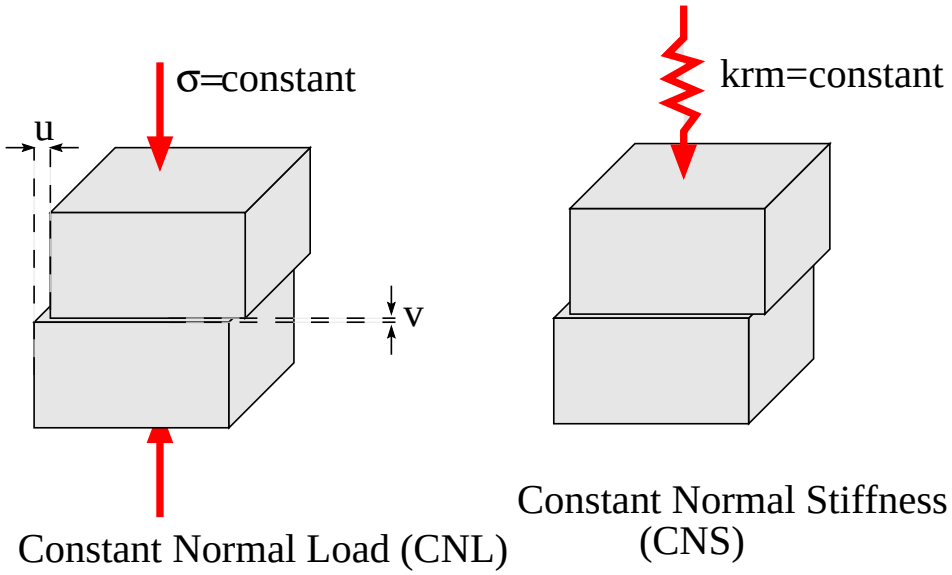

Figure 1: Cartoon depicting Constant Normal Load (CNL) and Constant Normal Stiffness (CNS) joint shear tests.

Tests were performed under variable constant normal stiffness (CNS). The results provided are somewhat limited however, with only detailed shear stress versus normal displacement results for two tests and peak shear versus peak normal stress for all tests.

The Olsson and Barton [2001] and Obert et al. [1976] data provide a consistent picture of joint behavior:

- Where sufficient data are provided, it is observed that joints *initially* undergo little dilation or even contract with increasing shear stress.
  - Fig. 11 in Obert et al. [1976] (Figure 5 in this work) shows one sample undergoing no dilation until about 1 MPa of shear stress, with the other sample contracting until about 5 MPa of stress.
  - Fig. 8 in Olsson and Barton [2001] (Figure 4 in this work) shows all samples slightly contracting until about 1 mm of shear displacement with essentially no change in normal stress (not shown in this figure).
- At low constant normal stiffness, joints quickly reach an initial peak shear stress and continue to dilate in the post-peak region
  - Fig. 11 in Obert et al. [1976] (Figure 5 in this work) shows a low CNL/CNS test dilating in the post-peak region.
  - Fig. 8 in Olsson and Barton [2001] (Figure 4 in this work) shows all CNS tests dilating after an initial break in the shear stress- shear displacement curve.
- As constant normal stiffness is increased, the ultimate joint strength increases.
  - In the case of the Olsson and Barton [2001] data, this can be linked to dilation which occurs after shear stress passes an initial, lower peak (See Figure 3).
  - In the Obert et al. [1976] data, the connection between dilation and the increase in confining stress at high CNS and an increase in shear strength is implied.

Lee et al. [2001] obtained measurements of dilation under CNL for multiple cycles of shear loading (see Figure 2). These figures show results for cyclic loading of rough granite joints. Consistent with the results obtained by Olsson and

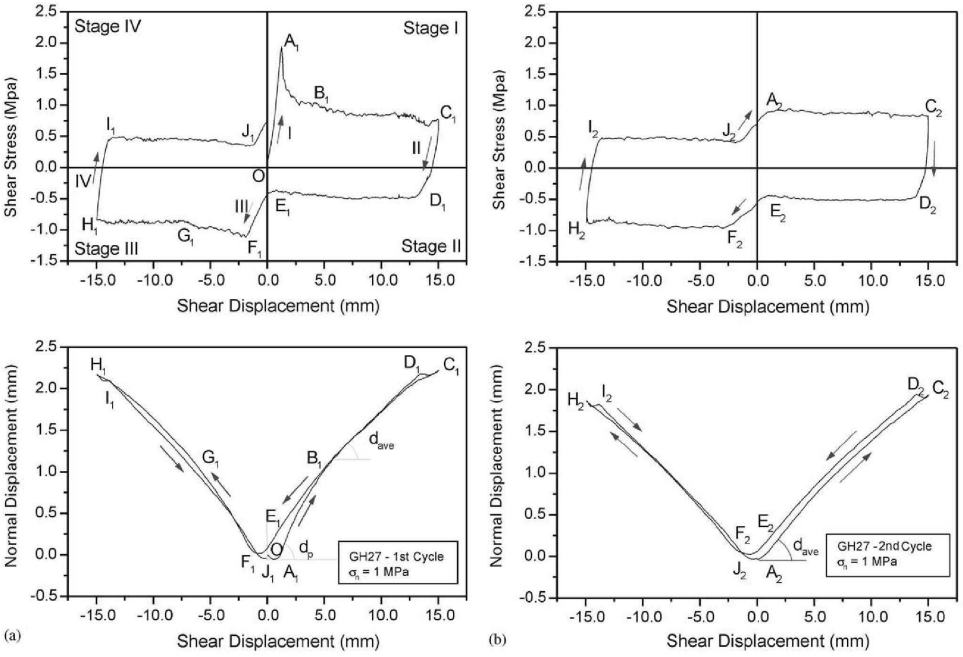

Fig. 8. Shear behaviors of rough granite joints for the first two cycles: (a) first cycle and (b) second cycle.

Figure 2: Figure 8 from Lee et al. [2001]. These figures show results for cyclic loading of rough granite joints. Note that the initial peak shear stress is reached at A_1 in the shear stress vs shear displacement plot, however the majority of the observed dilation occurs between A_1 and C_1 in the normal displacement vs shear displacement plot. The same type of behavior (without the initial peak shear stress) is observed upon sufficient shear in the opposite direction and for subsequent cycles.

Barton [2001], Lee et al. [2001] found that the majority of the observed dilation occurs after the initial peak shear stress is reached. The same type of behavior (without the initial peak shear stress) is observed upon sufficient shear in the opposite direction and for subsequent cycles of shear loading. In addition, the joint exhibits little dilation upon initial shear loading. Dilation becomes significant as the joint approaches peak shear stress.

1.3 Experiments Performed on Sandstone or Artificial Rock

In this section we review a portion of the available data from shear tests performed on non-granite specimens, including sandstones, tuff and artificial joints.

Fox et al. [1998] studied the cyclic loading of joints in tuff under CNL. Their results are similar to those obtained by Lee et al. [2001] for granite. In particular, the majority of the observed dilation occurred after the initial peak shear stress was reached. The same type of behavior (without the initial peak shear stress) was reproduced with sufficient shear in the opposite direction and for subsequent cycles of shear loading. Homand et al. [2001] and Huang et al. [1993] reported similar behavior for shear tests performed on artificial joints.

Leichnitz [1985] considered the shear deformation of sandstone joints under CNS and CNL. They report that very little dilation occurs upon initial shear loading of their joint specimens. Some dilation occurs before the joint starts to fail, however, their results indicate that the peak rate of dilation (instantaneous dilation angle) occurs as the joint starts to fail. The rate of dilation gradually drops to zero after 20 mm to 30 mm of shear displacement. Depending upon the combination of initial confining stress and confining stiffness, the ultimate strength of the joint occurred at initial break in slope of shear stress versus shear displacement or significantly later.

Lam and Johnston [1982] performed CNS tests on synthetic joints in the artificial "rock", "Johnstone." There samples were constructed with regular triangular asperities with and angle of 23° and a wavelength of 44.5 mm. Their measurements of dilation and normal stress typically show no dilation (some contract) of the joint for the first 0.5 mm to 1 mm of shear displacement. The results indicate small amounts of dilation prior to initial break in slope of shear stress versus shear displacement for some of the joints. Greatest rate of dilation with shear displacement typically occurred immediately after initial break in slope. The rate of dilation approached zero after between 2 mm and 8 mm of shear displacement, depending upon the final confining stress. The higher the final confining stress, the quicker the dilation approached its final value. As with Leichnitz [1985], Lam and Johnston [1982] found that the ultimate strength of the joint could be realized at the point of initial break in slope of shear stress versus shear displacement or later depending upon the combination of initial confining stress and confining stiffness.

Huang et al. [2002] performed CNL tests artificial joints with regular asperities using a material which was a mix of chalk, sand and water. The joints had matched triangular asperities with wavelength 20 mm and angles of 0°, 15°, and 30°. These

results show minimal dilation for between 0.5 mm to 1 mm of shear displacement, followed by significant dilation. This dilation occurs before significant break in slope of shear stress versus shear displacement and continues after the break in slope.

2 Review of Joint Models

The literature concerning joint models is extensive, providing a wide range of choices for the computational physicist. This section should not be regarded as a complete review, however, I have attempted to gather information on as many types of models as possible in order to describe the options available.

The following three sections describe the basic approaches taken when developing joint constitutive models.

2.1 Phenomenological-Type Models

Many models have been developed to reproduce specific experimental results with numerical considerations given a lower priority. Such approaches typically focus upon matching the results from a specific set of shear tests. By design, this approach will closely match available data. The difficulty is that, in practice, the loading conditions experienced by a joint will be more complicated than those exhibited in laboratory shear tests.

Heuze and Barbour [1982] developed a model intended to reproduce peak shear stress measurements from shear tests performed under CNL and CNS. This model assumes the joint dilates immediately upon shear displacement. In its simplest form, the dilation angle is constant until the joint fails, at which point the dilation angle becomes zero. In addition, the joint ceases to dilate if the confining stress exceeds a critical normal stress. When the joint fails the friction angle instantaneously drops from an initial value to a residual value. Although this model can approximate the peak shear stress behavior of joints under shear with CNL and CNS, it cannot reproduce the detailed shear stress vs shear displacment behavior as reported by Olsson and Barton [2001], Lee et al. [2001] and others (discussed in section 1.2).

Goodman [1980], p.164 presents an approach for predicting the shear response of a joint under constant normal displacement. This approach assumes a family of curves are available for shear tests under constant normal stress. Goodman [1980] argues that changing the confinement of the joint to constant normal displacement

corresponds to constantly moving from one constant normal stress test to another. Goodman [1980] assumes that the instantaneous dilation angle is zero (or very small) initially and reaches a peak approximately at peak shear stress after which it gradually drops.

Saeb and Amadei [1989] and Saeb and Amadei [1990] followed the spirit of the approach used by Goodman [1980] and developed a model where the behavior of the joint is tied explicitly to the combination of shear displacement and confining stress. For example, the presentation of their model starts with model curves of shear stress as a function of shear displacement for different values of confining stress. Key events in the shear tests occur at fixed values of shear displacement. For example, peak shear stress is achieved at a constant value of shear displacement (U_4 in Saeb and Amadei [1990]). Among the sample curves that Saeb and Amadei [1990] present for their model, all of them commence dilation immediately with any shear displacement (at U_0). In one of their examples, dilation ceases at peak stress (U_4), while in another example the dilation continues well beyond peak stress (until U_{14}).

2.2 Continuum-Theory Inspired Models

An alternative approach to developing a joint model is to build upon knowledge from continuum treatments of rock mechanics. The theoretical framework upon which such models are constructed is solid, however, it is sometimes difficult to relate the variables and parameters used by such models to the results of specific experiments.

For example, Plesha [1987] introduced a yield surface and plastic potential function to describe the response of the joint. This model was subsequently extended by Nguyen and Selvadurai [1998] to account for hydraulic behavior. Prior to yield, the joint response is elastic. When yielding, the displacement on the joint has an elastic and plastic component. These plastic components of displacement can include dilatant effects. In the model plastic deformation leads to degradation of the joint asperities and a reduction in friction angle. The theory leads to an elastoplastic stiffness matrix which contains gradients of the yield function and plastic potential.

Leichnitz [1985] developed a model which relates shear and normal stress increments to changes in shear and normal displacements via a stiffness matrix. The stiffness matrix has terms which are functions of the instantaneous dilation and friction angles. Their model fit to their own data suggests that the instantaneous dilation angle is zero initially and reaches a peak at the peak shear stress

after which it decays with increasing shear displacement.

Souley [1995] present a model which like that of Leichnitz [1985] relates the shear and normal stress increments to changes in shear and normal displacements using a stiffness matrix. The model of Souley [1995] is an extension of a simpler model (Saeb and Amadei [1992]) to include the effects of cyclic loading in normal and shear. Souley [1995] describe typical shear experiments (see their Figures 1(c) and 7(a)) as starting with little instantaneous dilation rate with peak dilation rate occurring at peak shear stress and then decreasing back to zero. They choose to approximate this behavior with a constant dilation angle (for constant confining stress) past peak until a residual state is reached. Souley [1995] assume that the pre-peak behavior of the joint is elastic. Consequently, a joint that is brought just short of peak shear stress can be returned to its initial state by reversing the direction of shear stress (see their Figure 7(b)). Their model is relatively easy to implement in two dimensions where shear direction is easy to define. In three dimensions the model becomes more difficult to implement.

2.3 Generalized Phenomenological Models

The continuously yielding joint model used in Itasca's 3DEC models yielding on the joint by employing the concept of plastic deformation. However, the details are less complicated than that of Plesha [1987]. The effective shear stiffness is modified as the shear strength is approached. A plastic displacement increment is calculated to be proportional to the ratio of current shear stress to current shear strength. Thus, unlike the model due to Plesha [1987], this model yields before the shear stress reaches the shear strength. An instantaneous friction angle is calculated and reduces due to damage from accumulated plastic displacement. The effective instantaneous dilatancy angle is related to the current and residual friction angles. This model exhibits peak rate of dilation near the peak shear stress with much lower dilation rate upon initial shear displacement.

2.4 The LDEC Joint Model

The basic idea of the LDEC model is to achieve a good fit to available data for joints in granite without introducing too many parameters or numerical pathology. This model is one similar to the simplest model implemented in 3DEC with a few improvements. The joint responds linearly in shear until the shear-strength envelope is exceeded (failure). Whenever the current stress state exceeds the shear-strength envelope, the stress is brought back onto the envelope and the joint slip is

incremented. The model will also *optionally* initiate slip at a given value of shear displacement, possibly before the shear strength is exceeded (This is to provide fit to observed data discussed later). The dilation force is increased in proportion to the joint slip increment. Consequently, once slip has occurred, the joint can experience an increase in confining stress and a corresponding increase in shear strength. The increment in dilation force decreases linearly to zero as the confining stress approaches a critical normal stress. With increasing slip, the tangent of the friction angle decreases linearly to a residual value. As currently implemented, it is assumed that slip (and dilation) is irreversible. Consequently, if a joint fails in shear, dilation occurs, however when the shear direction is reversed, the slip and dilation remain constant until the shear strength is exceeded in the opposite direction. As a result, the LDEC model does not reproduce the cyclic shear loading behavior observed by Lee et al. [2001] where the joint contracts with the reversal of shear load direction.

The joint strength is assumed to be a function of the current confining stress:

$$\tau_s = C + \sigma_n \tan(\phi_0 + \phi_1) \tag{1}$$

Where C is the shear cohesion (typically zero), σ_n is the *current* normal stress and ϕ_0 and ϕ_1 are friction angles. The joint response is linear until the increment in shear stress would take it beyond τ_s.

At each time step an elastic increment in shear stress is calculated using:

$$d\tau = K_s du \tag{2}$$

where $d\tau$ is the shear stress increment and du is the shear displacement increment. If the increment in shear stress results in the shear stress remaining less than the shear strength (τ_s) nothing else is done. However, if the new shear stress would exceed τ_s the joint is assumed to have undergone some plastic deformation we will call "shear slip" or $d\mathcal{S}$. The shear stress is returned to τ_s and a shear slip increment is calculated to be the fraction of the shear displacement that was responsible for taking the shear stress belong τ_s:

$$d\mathcal{S} \leftarrow (\tau - \tau_s) / d\tau \tag{3}$$

$$\tau \leftarrow \tau_s \tag{4}$$

In the LDEC model, when the joint slips it will attempt to dilate. Because LDEC is an explicit code, opening of the joint can only occur by physically moving the adjacent blocks. Consequently, we model dilation by increasing the normal

stress on the joint. This will tend to force the adjacent blocks apart and attempt to open the joint. If the surrounding blocks are under constant normal stress the joint will dilate to its maximum extent. If the surrounding blocks are under constant normal stiffness, then the confining stress on the blocks will increase as the joint attempts to dilate and a new equilibrium opening dilation will be achieved, less than the opening realized for constant normal stress. Most importantly, if the joint is confined under constant normal stiffness, the dilation will result in increased normal stress and, potentially, increased shear strength. Consequently, the peak shear stress observed can occur after the joint has experienced some shear slip.

The dilation in the absence of confinement is related to the slip by:

$$dv = (1 - \sigma_{cr}/\sigma_n) \tan\psi_0 d\mathcal{S} \tag{5}$$

where dv is the potential increment in joint opening. Here, ψ_0 is the initial dilation angle and σ_{cr} is the critical normal stress above which dilation will not occur. This can be thought of as the confining stress at which asperities are sheared off. As explained above, the joint is not actually opened this amount, but this increment is used to calculate an increase in stress on the joint:

$$d\sigma_n = K_n (1 - \sigma_{cr}/\sigma_n) \tan\psi_0 d\mathcal{S} \tag{6}$$

and the surrounding blocks respond by attempting to move apart and open the joint. The dilation force increases according to this equation until the amount of slip reaches a limiting value, $\mathcal{S}_L$.

As the joint slips, the friction angle is also reduced to model the observed softening of joints:

$$d\phi_1 = d\mathcal{S} / (\mathcal{S}_R - \mathcal{S}) \tag{7}$$

where $\mathcal{S}_R$ is the value of slip at which the friction angle $(\phi_0 + \phi_1)$ reverts to the residual value ϕ_0.

Some experimental studies show joints dilating during the initial linear elastic response portion of the joint behavior after some initial shear displacement has occurred. To model this behavior with LDEC model we have included an optional slip initialization parameter, u_I. When this option is enabled and the shear displacement exceeds u_I, the shear slip increment is given by:

$$d\mathcal{S} = \tau/\tau_s du \tag{8}$$

when $\tau < \tau_s$ and

$$d\mathcal{S} = du \tag{9}$$

when $\tau > \tau_s$.

u	Shear displacement
$\mathcal{S}$	Shear slip
v	Normal displacement
τ	Shear stress
τ_s	Current shear strength
σ_n	Normal stress

Table 1: Variables used by LDEC model.

C	Shear cohesion
ϕ_0	Residual friction angle
ϕ_1	Initial additional friction angle
ψ_0	Initial dilation angle
K_n	Current normal stiffness (potentially nonlinear)
K_s	Shear stiffness
σ_{cr}	Critical normal stress
$\mathcal{S}_L$	Limiting shear slip for dilation to occur
$\mathcal{S}_R$	Shear slip at which friction angle drops to residual value
u_I	*Optional* shear displacement at which slip (and dilation) starts

Table 2: Parameters used in LDEC model

3 LDEC Model Fit to Granite Data

In this section a single set of parameters (see Table 3) were used to reproduce the CNS and CNL data of Olsson and Barton [2001] and the CNS data due to Obert et al. [1976]. The data published by Olsson and Barton [2001] are more detailed than Obert et al. [1976]. In particular, Olsson and Barton [2001] provide shear stress and dilation as a function of shear displacement, while Obert et al. [1976] provide peak shear stress and limited shear vs normal displacement information. The approach taken was choose parameters to fit the LDEC model to the Olsson and Barton [2001] data and see what results this *same* set of parameters give when emulating the tests performed by Obert et al. [1976].

C	0 Pa
ϕ_0	35
ϕ_1	10
ψ_0	9.1
K_n	30 GPa/m
α_j	1 mm
K_s	3 GPa/m
σ_{cr}	20 MPa
$\mathcal{S}_L$	15 mm
$\mathcal{S}_R$	2 mm
u_I	1 mm

Table 3: Parameters used in LDEC model

3.1 LDEC Model Fit to Olsson and Barton [2001]

The details of the LDEC model and parameters are described in section 2.4. First we consider the Olsson and Barton [2001] plots for shear stress vs shear displacement (Fig. 3). The initial linear response has a slope of approximately 3 MPa/mm or 3 GPa/m. This corresponds to our choice of K_s.

In the same figure we see that the zero stiffness, $\sigma_n = 2$ MPa case initially fails at about 2.25 MPa and relaxes to a residual shear stress of about 1.75 MPa after about 2 mm of shear slip. This suggests an initial friction angle of $\text{atan}(2.25/2) = 48.4$ and residual friction angle of $\text{atan}(1.75/2) = 41.1$. These values seem rather high so instead we compromise with $\phi_0 = 35$ and $\phi_1 = 10$. The amount of slip to residual corresponds to our $\mathcal{S}_L$. We also assume that $C = 0$.

If we consider the plots of normal displacement vs shear displacement (Fig. 4) we can determine most of the other parameters of interest. In particular, the zero confining stiffness case corresponds to maximum dilation with no increase in confining stress. This case shows an opening of about 2.25 mm over 14 mm of shear displacement. This suggests a dilation angle of $\text{atan}(2.25/14) = 9.1$ degrees. The increase in normal displacement gradually flattens out with increasing shear slip and we assume that we can approximate its behavior by letting it reach a maximum at a slip of 15 mm (which becomes our choice for $\mathcal{S}_L$. Interestingly, all results obtained by Olsson and Barton [2001] showed dilation to start at 1 mm of shear displacement even though for the high confining stress case the response of the joint was close to linear up to 1.5 mm of shear displacement (Fig. 3). Consequently, we take $u_I = 1$ mm.

We assume that above 20 MPa of confining stress the joint cannot dilate due to shearing of the asperities (σ_{cr}). In summary, the choice of parameters suggested by the Olsson and Barton [2001] data are in Table 3.

The fit obtained by using the LDEC model with these parameters is shown in Figures 3 and 4.

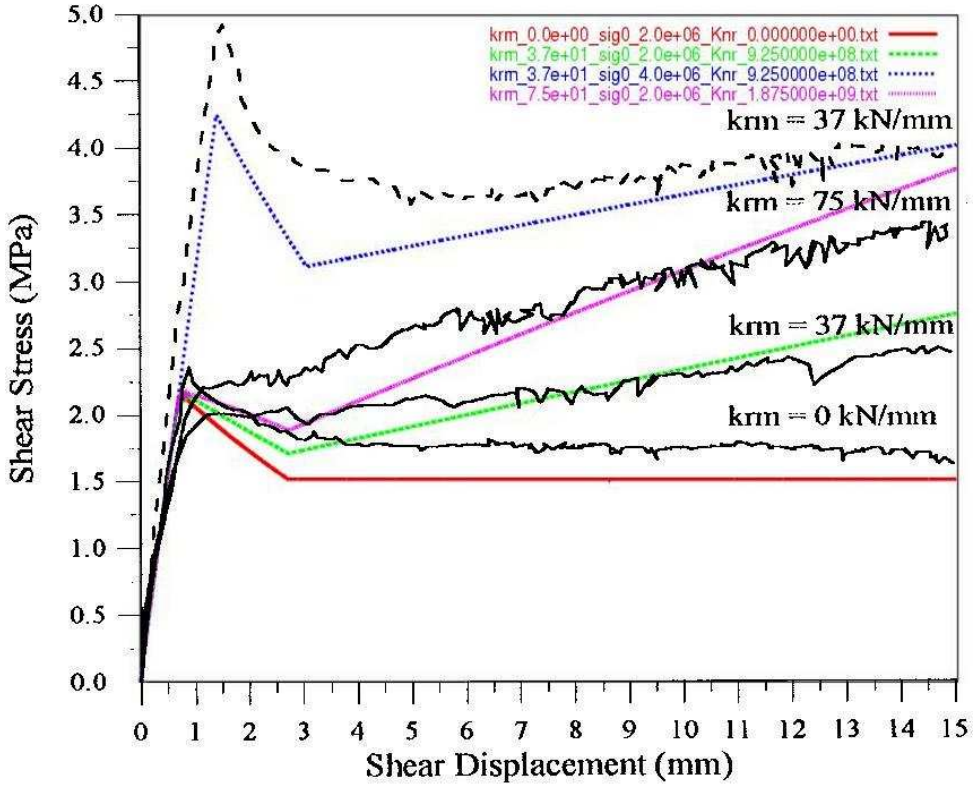

Figure 3: Comparison between shear stress vs shear displacement for the LDEC model and Olsson and Barton [2001], Fig. 7. The black lines are experimental results and color lines are from LDEC simulations using the LDEC model. The dashed line corresponds to a test with 4 MPa initial confining stress. The solid lines have 2 MPa initial confining stress with increasing levels of CNS. The peak shear stress and post-peak behaviors are mostly well captured by the LDEC model. Note that the 4 MPa test case, according to Olsson and Barton [2001], was a rougher fracture and consequently the model does not match its peak stress as well as the other tests. In particular, we see that the shear tests for 2 MPa show no increase in the stress at which the break in slope occurs. The immediate post-initial-peak behavior of the high CNS tests is not well reproduced by the simplistic LDEC model.

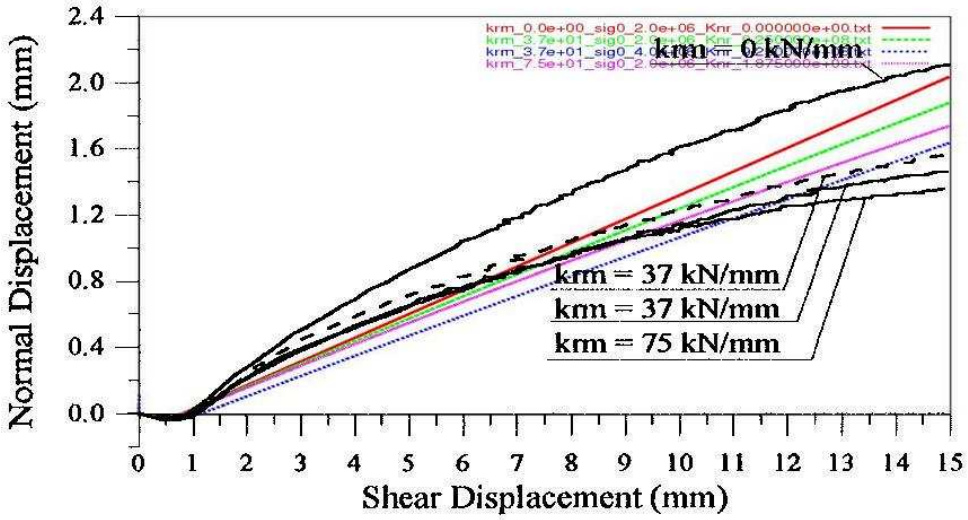

Figure 4: Comparison between dilation vs shear displacement for the LDEC model and Olsson and Barton [2001], Fig. 8. The black lines are experimental results and color lines are from LDEC simulations using the LDEC model. The dashed line corresponds to a test with 4 MPa initial confining stress. The solid lines have 2 MPa initial confining stress with increasing levels of CNS. The LDEC model has the expected trends and reproduces most of the trends in the data. In particular, the highest CNS case of 75 kN/mm is predicted to have the least dilation overall. The LDEC model also predicts that the 4 MPa-37 kN/mm test (blue curve) will have less dilation than the 2 MPa-37 kN/mm test (green curve) as we would expect. However, the actual experiment shows the opposite: The higher confining stress leads to more dilation. This again is probably attributable to the sample for the 4 MPa-37 kN/mm being rougher.

3.2 Comparison with Obert et al. [1976]

The Obert et al. [1976] data is not as detailed as that of Olsson and Barton [2001]. In particular, the evolution of shear stress with shear displacement is not provided and very little explicit normal displacement data is given. However, Obert et al. [1976] provide plots of peak shear stress vs peak normal stress for a number of tests under different levels of confining stiffness. The data implies that increasing confining stiffness leads to increased confining stress as the joint attempts to dilate, leading to a stronger joint.

In order to see if the Obert et al. [1976] data were *quantitatively* consistent with the Olsson and Barton [2001] data, numerical tests were performed which reproduced the experiments of Obert et al. [1976] using the same model parameters as were used to fit the Olsson and Barton [2001] data.

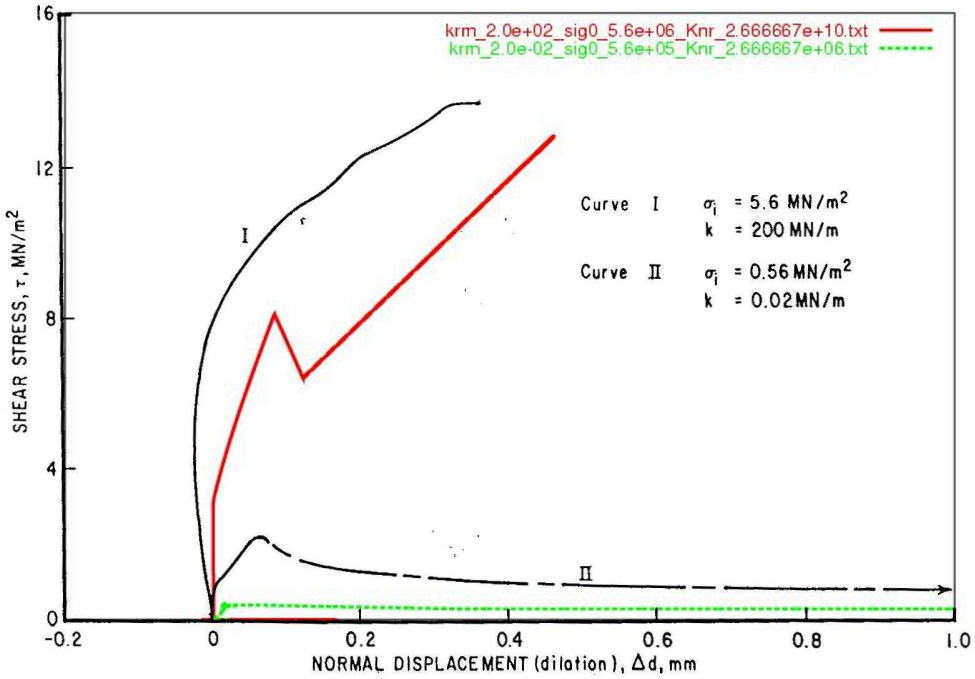

Figure 5: Comparison between the LDEC model and Obert et al. [1976], Fig. 11. Obert et al. [1976] provide shear stress vs normal displacement data for only two tests on fractured granite. The lower CNS test shows no dilation with initial application of shear stress. As the peak shear stress is approached, the joint starts to dilate. Post-peak the joint continues to dilate. For the high CNS test the joint actually contracts and does not dilate until about 5 MPa of shear stress develops. The LDEC model fit to the Olsson and Barton [2001] data qualitatively reproduces these results. The simple LDEC approach to softening the friction angle post-initial-peak results in the "zig-zag" feature.

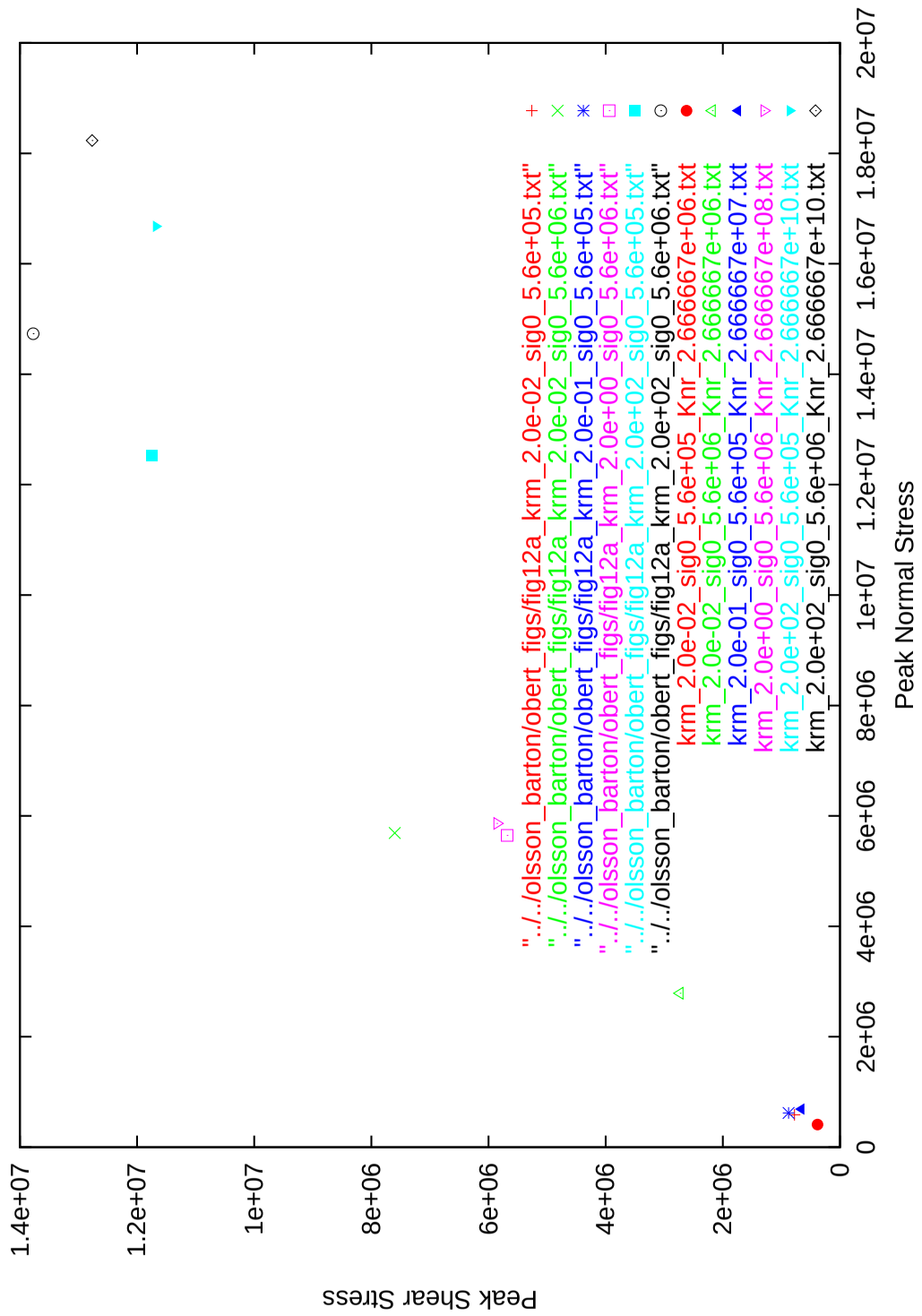

Figure 6: Comparison between the LDEC model and Obert et al. [1976], Fig. 12. The first six entries in the legend correspond to the peak shear vs peak normal stress obtained by Obert et al. [1976]. The last six entries are the corresponding results obtained with the LDEC model fit to the Olsson and Barton [2001] data. Points of the same color, but with a different symbol, correspond to the same conditions. Ideally all pairs of same color points would coincide. Most of the LDEC model results are close to the measurements of Obert et al. [1976] with one exception. The green × symbol corresponds to what Obert et al. [1976] obtained for a rock-mass stiffness of 2e-02 MN/m and initial confining stress of 5.6e6 Pa. This sample has a higher peak stress than that obtained for 2e-01 MN/m and initial confining stress of 5.6e6 Pa (the blue asterisk), suggesting that the green × may be a particularly rough joint.

4 Conclusion

The LDEC model presented is relatively simple and yet is capable of reproducing the main features of the granite data obtained by Obert et al. [1976] and Olsson and Barton [2001] with the *same* choice of parameters.

As currently implemented, it is assumed that slip (and dilation) is irreversible. Consequently, if a joint fails in shear, dilation occurs, however when the shear direction is reversed, the slip and dilation remain constant until the shear strength is exceeded in the opposite direction. As a result, the LDEC model does not reproduce the cyclic shear loading behavior observed by Lee et al. [2001] where the joint contracts with the reversal of shear load direction. If it is demonstrated that this effect is important in problems of interest, the LDEC model can be extended to allow slip and dilation to be reversible.

References

D. J. Fox, D. D. Kana, and S. M. Hsiung. Influence of interface roughness on dynamic shear behavior in jointed rock. *In. J. Rock Mech. Min. Sci.*, 35(7): 923–940, 1998.

R. E. Goodman. *Introduction to Rock Mechanics*. John Wiley & Sons, 1980.

F. E. Heuze and T. G. Barbour. New models for rock joints and interfaces. *Journal of Geotechnical Engineering: Proceedings of the ASCE*, 108(GT5), 1982.

F. Homand, T. Belem, and M. Souley. Friction and degradation of rock joint surfaces under shear loads. *Int. J. Numer. Anal. Meth. Geomech.*, 25:973–999, 2001.

T. H. Huang, C. S. Change, and C. Y. Chao. Experimental and mathematical modeling for fracture of rock joint with regular asperities. *Engineering Fracture Mechanics*, 69:1977–1996, 2002.

X. Huang, B. C. Haimson, M. E. Plesha, and X. Qiu. An investigation of the mechanis of rock joints - Part I. laboratory investigation. *Int. J. Rock Mech. Min. Sci. & Geomech. Abstr.*, 30(3):257–269, 1993.

T. S. K. Lam and I. W. Johnston. A constant normal stiffness direct shear machine. *Proceedings of the Seventh Southest Asian Geotechnical Conference*, pages 805–820, 1982. 22-26 November, Hong Kong.

H. S. Lee, Y. J. Park, T. F. Cho, and K. H. You. Influence of asperity degradation on the mechanical behavior of rough rock joints under cyclic shear loading. *Int. J. Rock Mech. & Mining Sci.*, 38:967–980, 2001.

W. Leichnitz. Mechanical properties of rock joints. *Int. J. Rock Mech. Min Sci & Geomech. Abstr.*, 22(5):313–321, 1985.

T. S. Nguyen and A. P. S. Selvadurai. A model for coupled mechanical and hydraulic behavior of a rock joint. *Int. J. Numer. Analyt. Meth. Geomech.*, 22: 29–48, 1998.

L. Obert, B. T. Brady, and F. W. Schmechel. The effect of normal stiffness on the shear resistance of rock. *Rock Mechanics*, 8:57–72, 1976.

R. Olsson and N. Barton. An improved model for hydromechanical coupling during shearing of rock joints. *International Journal of Rock Mechanics & Mining Sciences*, 38:317–329, 2001.

M. E. Plesha. Constitutive models for rock discontinuities with dilatancy and surface degradation. *Int. J. Numer. Analyt. Meth. Geomech.*, 11:345–362, 1987.

S. Saeb and B. Amadei. Effect of boundary conditions on the shear behavior of a dilatant rock joint. *Rock Mechanics as a Guide for Efficient Utilization of Natural Resources: Proceedings of the 30th U.S. Symposium*, pages 107–114, 1989. Khai (ed.), Balkema, Rotterdam, ISBN 90 6191 871 5.

S. Saeb and B. Amadei. Modelling joint response under constant or variable normal stiffness boundary conditions. *Int. J. Rock. Mech. Min. Sci. & Geomech. Abstr.*, 27(3):213–217, 1990.

S. Saeb and B. Amadei. Modelling rock joints under shear and normal loading. *Int. J. Rock Mech. Min. Sci. & Geomech. Abstr.*, 29:267–278, 1992.

M. Souley. An extention to the saeb and amadei constitutive model for rock joints to include cyclic loading paths. *Int. J. Rock Mech. Min. Sci. & Geomech. Abstr.*, 32(2):101–109, 1995.